

Supporting Material for
Modeling of Cardiac Muscular Thin Films:
Pre-stretch, Passive and Active Behavior

Jongmin Shim¹, Anna Grosberg², Janna C. Nawroth³,
Kevin Kit Parker², and Katia Bertoldi¹

¹*School of Engineering and Applied Science, Harvard University, Cambridge, MA*

²*Disease Biophysics Group, Wyss Institute for Biologically Inspired Engineering, School of Engineering
and Applied Science, Harvard University, Cambridge, MA*

³*Division of Biology, California Institute of Technology, Pasadena, CA*

S1 Experimental Methods

This section provides a detailed description of the preparation of the silicone thin film and cell harvesting procedure.

S1.1 Manufacturing the Silicone Thin Films

The silicone thin films were prepared via a multi-step spin coating process, extending a previously published method (Feinberg et al., 2007) in order to allow for higher experimental throughput. The samples prepared this way have been dubbed “Heart on a chip”. To prepare the chips, a section of glass ($7.5\text{cm} \times 11\text{cm}$) was sonicated and covered with a protective film (Static Cling Film, McMaster-Carr, Robbinsville, NJ) on both sides. Rectangles ($1\text{cm} \times 0.6\text{cm}$) were cut out of the top protective film, and poly(N-isopropylacrylamide) (PIPAAm, Polysciences, Inc., Warrington, PA) in 1-butanol (10% *w/v*) was spin-coated onto the uncovered portions of the glass, and then the top protective film was removed. The silicone polymer polydimethylsiloxane (PDMS, Sylgard 184-Dow Corning, Midland, MI) was pre-cured for 1 to 6 hours, spin coated onto the glass, and cured for 8 hours at 65°C . The bottom protective film was removed, and the glass section was cut into cover slips of $1.4\text{cm} \times 1.2\text{cm}$. From each glass section, two cover slips were used to measure the thickness of the PDMS layer using a profilometer (Dektak 6M, Veeco Instruments Inc., Plainview, NY). The PDMS surface of the cover slip was functionalized and sterilized for 8 minutes in UV ozone (Model No. 342, Jetlight Company, Inc., Phoenix, AZ). Fibronectin (FN, Sigma, St. Louis, MO or BD Biosciences, Sparks, MD) was micropatterned onto the surface via microcontact printing with a brick patterned PDMS stamp (each brick was $20\mu\text{m}$ wide and $100\mu\text{m}$ long, and each short edge terminated with $5\mu\text{m}$ long saw-tooth, Bray et al., 2008), such that the brick pattern would be perpendicular or at some tilted angle to the long edge of the cover slip. The gaps in the pattern were blocked by incubating the cover slip in Pluronic F127 (BASF Group, Parsippany, NJ) for 5 minutes, and then the chips were stored at 4°C until cell seeding. Three different PDMS thickness were made through this procedure: $14.5\mu\text{m}$, $18.0\mu\text{m}$, $23.0\mu\text{m}$.

S1.2 Cell harvesting, Seeding, and Culture

Cell harvesting was conducted in accordance with the guidelines of Institutional Animal Care and Use Committee of Harvard University. Cardiomyocytes were harvested and isolated based on published protocols (Adams et al., 2007). Briefly, ventricles were extracted from two-day-old neonatal Sprague-Dawley rats (Charles River Laboratories, Wilmington, MA) and homogenized by washing in Hanks balanced salt solution, then incubated with trypsin overnight at 4°C . To release the myocytes into solution, the ventricular tissue was digested with collagenase at 37°C . Cells were re-suspended in M199 culture medium supplemented with 10% (*v/v*) heat-inactivated fetal bovine serum (FBS), 10mM HEPES, 3.5g/L glucose, 2mM L-glutamine, 2mg/L vitamin B-12, and 50U/ml penicillin. The myocytes were seeded on the substrates at a density of 400,000 cells per cover slip (round, diameter of 18mm), and cultured for a period of four days prior to running the assay. During the initial 48 hours, the cells were kept at 37°C and $5\%\text{CO}_2$ with 10% FBS media in the culture; thereafter, the maintenance media (2% FBS) was used. The measured cell thickness was approximately $4.0\mu\text{m}$.

S1.3 Contractility Experiments

To run the contractility experiments, the chip was moved to a Petri dish with 37°C normal Tyrode's solution (1.192g of HEPES, 0.901g of glucose, 0.265g of CaCl_2 , 0.203g of MgCl_2 , 0.403g of KCl , 7.889g of NaCl , and 0.040g of NaH_2PO_4 per liter of deionized water; reagents from Sigma, St. Louis, MO). The PDMS elastic layer was cut such as to leave the PDMS along the border of the cover slip intact, while in the center there were two rows of three to four rectangles (approximately $2\text{mm} \times 3.5\text{mm}$) separated by approximately 1mm , and connected to the PDMS border by one edge (see Fig. 2A). The unwanted film was peeled away, exposing the temperature-sensitive PIPAAm beneath the rectangular strips and causing it to dissolve as the solution was allowed to cool down towards room temperature. Subsequently, the rectangular films were free to move vertically up from the plane of the cell culture, without completely separating from the chip. The chip with six or eight rectangular films was moved to a heated bath ($34^\circ\text{C} - 37^\circ\text{C}$) under a stereomicroscope (Model MZ6 with darkfield base, Leica Microsystems, Inc., Wetzlar, Germany), and the dynamics of the films was recorded from above at 120 *frames/sec* (Basler A602f camera, Exton, PA). Several snapshots from the recorded movies are shown in Figs. 2A and 2E.

While the film laid flat on the glass, both its length and width were measured. As the films contracted away from the surface, the horizontal projection was recorded. Unimpeded films would first isometrically deform to a curvature corresponding to the diastolic tension in the cells, and then continue to deform until peak systole. For substrates with cells aligned with the length of the film, the observed deformation was a shortening of the projection, described in Fig. 1C (top). On the other hand, the substrates with cells at an angle to the length of the film showed the inclined free edge of the film (see Fig. 1C (bottom)), so an appropriate projection length needed to be defined in order to obtain the curvature of the MTFs. To ensure all films on the chip were moving at once, the myocytes were field-stimulated at 1.5Hz with 5 to 20V using an external field stimulator (Myopacer, IonOptix Corp., Milton, MA) which applied a 10msec square wave pulse.

S2 Constitutive Equations for Bio-hybrid Films

In this section, we first summarize the equations governing the nonlinear deformation of hyperelastic materials, following the formulation previously introduced by Bergström and Boyce (1998). Then, the equations are specialized to capture the behavior of the elastomeric substrate and the cardiac myocytes. As mentioned in Section 1, cardiac myocytes comprise highly aligned myofibrils, so their behavior is captured extending the formulation previously developed to model fiber reinforced elastomers (Spencer, 1984).

S2.1 General Formulation

Let $\mathbf{F} = \partial\mathbf{x}/\partial\mathbf{X}$ be the deformation gradient mapping a material point from the reference position \mathbf{X} to its current position \mathbf{x} , and $J = \det\mathbf{F}$ be its determinant. The behavior of nearly incompressible materials is effectively described by splitting the deformation locally into volumetric (denoted by superscript v) and isochoric (denoted by superscript i) components as

$$\mathbf{F} = \mathbf{F}^v \cdot \mathbf{F}^i, \quad \text{where } \mathbf{F}^v = J^{1/3}\mathbf{1}, \quad \mathbf{F}^i = J^{-1/3}\mathbf{F}. \quad (\text{S1})$$

For an isotropic hyperelastic material, the strain energy density ψ is a function of the three invariants of $\mathbf{C} = \mathbf{F}^T \cdot \mathbf{F}$, $\psi = \psi(I_1, I_2, I_3)$. Based on the kinematic assumption (S1), a decoupled

form for ψ is introduced

$$\psi = \psi^v(J) + \psi^i(\bar{I}_1, \bar{I}_2), \quad (\text{S2})$$

with

$$\bar{I}_1 = \text{tr} \mathbf{C}^i, \quad \bar{I}_2 = \frac{1}{2} \left[(\text{tr} \mathbf{C}^i)^2 - \text{tr} (\mathbf{C}^{i2}) \right]. \quad (\text{S3})$$

When an isotropic material is reinforced by a family of fibers with direction \mathbf{a}_0 in the reference configuration, the isochoric part of the strain energy can be expressed as a function of not only \bar{I}_1 and \bar{I}_2 , but also two additional invariants (\bar{I}_4, \bar{I}_5) depending on \mathbf{a}_0 (Spencer, 1984),

$$\psi^i = \psi^i(\bar{I}_1, \bar{I}_2, \bar{I}_4, \bar{I}_5), \quad (\text{S4})$$

with

$$\bar{I}_4 = \mathbf{a}_0 \cdot \mathbf{C}^i \cdot \mathbf{a}_0 = \bar{\lambda}^2, \quad \bar{I}_5 = \mathbf{a}_0 \cdot \mathbf{C}^{i2} \cdot \mathbf{a}_0. \quad (\text{S5})$$

However, the dependence of the material response on \bar{I}_2 or \bar{I}_5 is generally weak, so that the isochoric part of the strain energy can be simplified as

$$\psi^i = \psi_{iso}^i(\bar{I}_1) + \psi_{ani}^i(\bar{I}_4), \quad (\text{S6})$$

where ψ^i is further decoupled into the isotropic contribution (ψ_{iso}^i) and the anisotropic contribution (ψ_{ani}^i).

Finally, the Cauchy stress \mathbf{T} is found by differentiating ψ with respect to \mathbf{C} as

$$\mathbf{T} = \frac{2}{J} \mathbf{F} \frac{\partial \psi}{\partial \mathbf{C}} \mathbf{F}^T = \frac{\partial \psi^v}{\partial J} \mathbf{1} + \frac{2}{J} \left[\frac{\partial \psi_{iso}^i(\bar{I}_1)}{\partial \bar{I}_1} \text{dev}(\mathbf{B}^i) + \bar{I}_4 \frac{\partial \psi_{ani}^i(\bar{I}_4)}{\partial \bar{I}_4} \text{dev}(\bar{\mathbf{a}} \otimes \bar{\mathbf{a}}) \right], \quad (\text{S7})$$

where “dev” stands for deviatoric part of 2^{nd} order tensors, $\mathbf{B}^i = \mathbf{F}^i \cdot \mathbf{F}^{iT}$ is the left Cauchy-Green tensor, and $\bar{\mathbf{a}} = \mathbf{F}^i \cdot \mathbf{a}_0 / \sqrt{\bar{I}_4}$ is the unit directional vector of fiber in the deformed configuration. In the following two sections, the above general formulation is specialized to capture the behavior of the elastomeric substrate and the cardiac myocytes.

S2.2 Elastomeric Substrate

The elastomeric substrate is fabricated using PDMS, and its behavior is well captured using a neo-Hookean model. A decoupled form of strain energy density is given by:

$$\psi = \psi^v(J) + \psi^i(\bar{I}_1) = \frac{\tilde{\kappa}}{2} (J - 1)^2 + \frac{\tilde{E}}{6} (\bar{I}_1 - 3), \quad (\text{S8})$$

where $\tilde{\kappa}$ and \tilde{E} denote the bulk modulus and the initial elastic modulus of the elastomer, respectively. Based on Eq. (S7), the Cauchy stress is obtained as:

$$\mathbf{T} = \tilde{\kappa}(J - 1)\mathbf{1} + \frac{\tilde{E}}{3J} \text{dev}(\mathbf{B}^i). \quad (\text{S9})$$

S2.3 Cardiac Muscle Cell

This paper presents a 3-D phenomenological model that captures the two major features of cardiac muscles: the passive behavior including pre-stretched deformation and their active behavior including systole and diastole. This subsection presents a detailed derivation of the constitutive equations for the passive and active behavior while the kinematics including pre-stretch is provided in Section 3.2.

In order to describe both passive (representing resting status) and active (including systole and diastole) behavior of cardiomyocytes, we specify a decoupled form of free energy as:

$$\psi = \psi^v(J) + \psi_{iso}^i(\bar{I}_1) + \psi_{ani}^{ip}(\bar{I}_4) + \psi_{ani}^{ia}(\bar{I}_4, q), \quad (\text{S10})$$

where q is the activation level of cardiac muscle cells. In the present model, while ψ^v and ψ_{iso}^i reflect the volumetric and the isotropic contribution of the intercellular part, respectively, ψ_{ani}^{ip} and ψ_{ani}^{ia} represent the passive and the active contributions of anisotropic effect of the myofibril, respectively.

Here, as for the elastomeric substrate, the volumetric free energy term is chosen as

$$\psi^v(J) = \frac{\hat{\kappa}}{2} (J - 1)^2, \quad (\text{S11})$$

and the isotropic contribution of the intercellular part is captured using a neo-Hookean formulation

$$\psi_{iso}^i = \frac{\hat{E}_c}{6} (\bar{I}_1 - 3), \quad (\text{S12})$$

where $\hat{\kappa}$ denotes the bulk modulus of the cells and \hat{E}_c is the initial elastic modulus of intercellular part. Several experimental studies (Le Guennec et al., 1990; Granzier and Irving, 1995; Palmer et al., 1996; Cazorla et al., 2000; Weiwad et al., 2000; Boron and Boulpaep, 2009) reveal that the passive response of cardiac cells is characterized by an exponential relation between stress and deformation (see Fig. 3A). In order to capture such behavior of cardiac cells, we propose the following free energy

$$\psi_{ani}^{ip}(\bar{\lambda}) = \frac{\hat{E}_p}{\hat{\alpha}^2} \left[e^{\hat{\alpha}(\bar{\lambda}-1)} - \hat{\alpha}(\bar{\lambda}-1) - 1 \right], \quad (\text{S13})$$

where $\bar{\lambda} = \sqrt{\bar{I}_4}$, \hat{E}_p is the initial elastic modulus, and $\hat{\alpha}$ characterizes the monotonically increasing slope of the stress-strain relation of the passive response of the fibers. For the active response (see Fig. 3B), a bell-type relation between stress and deformation was shown by several studies (Zajac, 1989; Weiwad et al., 2000; Boron and Boulpaep, 2009). Here, we simplify the active stress-stretch relation into a quadratic form, which is captured introducing the following free energy

$$\psi_{ani}^{ia}(\bar{\lambda}, q) = \begin{cases} \frac{\hat{P}q}{2(1-\hat{\lambda}_o)^2} \left[2(1-2\hat{\lambda}_o) \ln \bar{\lambda} + (4\hat{\lambda}_o - \bar{\lambda} - 1)(\bar{\lambda} - 1) \right], & \text{if } 1 < \bar{\lambda} < (2\hat{\lambda}_o - 1), \\ 0, & \text{otherwise,} \end{cases} \quad (\text{S14})$$

where \hat{P} is the isometric twitch stress (*i.e.*, the maximum contraction force per unit cross-sectional area) and $\hat{\lambda}_o$ is the optimal stretch (*i.e.*, the stretch at which the maximum active stress is attained). Since Fig. 2B-D and F clearly show that diversity in cell conditions causes

large variations of the peak amplitudes, a range of values for \hat{P} will be identified to account for biological variability. Finally, the activation level q is a function of time and is defined as

$$q(t) = \left(\frac{t}{\hat{T}}\right)^2 \exp\left[1 - \left(\frac{t}{\hat{T}}\right)^2\right], \quad (\text{S15})$$

where \hat{T} is the characteristic contraction time.

Based on Eq. (S7), the proposed free energy results in the following Cauchy stress

$$\mathbf{T} = \mathbf{T}^v + \mathbf{T}_{iso}^i + \mathbf{T}_{ani}^{ip} + \mathbf{T}_{ani}^{ia}, \quad (\text{S16})$$

where

$$\mathbf{T}^v = \hat{\kappa}(J - 1)\mathbf{1}, \quad (\text{S17})$$

$$\mathbf{T}_{iso}^i = \frac{\hat{E}_c}{3J} \text{dev}(\mathbf{B}^i), \quad (\text{S18})$$

$$\mathbf{T}_{ani}^{ip} = \frac{\hat{E}_p \bar{\lambda}}{\hat{\alpha} J} \left[e^{\hat{\alpha}(\bar{\lambda}-1)} - 1 \right] \text{dev}(\bar{\mathbf{a}} \otimes \bar{\mathbf{a}}), \quad (\text{S19})$$

$$\mathbf{T}_{ani}^{ia} = \begin{cases} \frac{\hat{P}q}{J} \left[1 - \left(\frac{\bar{\lambda} - \hat{\lambda}_o}{1 - \hat{\lambda}_o} \right)^2 \right] \text{dev}(\bar{\mathbf{a}} \otimes \bar{\mathbf{a}}), & \text{if } 1 < \bar{\lambda} < (2\hat{\lambda}_o - 1), \\ 0, & \text{otherwise.} \end{cases} \quad (\text{S20})$$

S3 Parameter Identification for the Constitutive Model

This section presents the procedure to identify the 11 material parameters entering into the proposed 3-D constitutive model. While the material parameters for the elastomeric substrate are provided by the manufacturers, the parameters needed for the cardiac muscle cell response are obtained from literature and contraction assays performed with neonatal rat ventricular myocytes micropatterned on PDMS thin films.

S3.1 Summary of Model Parameters

The proposed constitutive model requires 11 material constants:

- Elastomeric substrate
 - \tilde{E} Initial elastic modulus
 - $\tilde{\kappa}$ Initial bulk modulus
- Pre-stretched deformation of cardiac muscle cells
 - $\hat{\theta}$ Angle defining the initial alignment of the cells within the $x_1 - x_2$ plane
 - $\hat{\lambda}_S$ Pre-stretch developed in the cardiomyocytes during cell maturation
- Volumetric and isotropic behavior of cardiac muscle cells
 - \hat{E}_c Initial elastic modulus of intercellular part
 - $\hat{\kappa}$ Initial bulk modulus
- Passive fiber behavior of cardiac muscle cells
 - \hat{E}_p Initial elastic modulus of fiber
 - $\hat{\alpha}$ Constant related to the slope of stress-strain relation of passive fiber

- Active fiber behavior of cardiac muscle cells
 - \hat{P} Isometric twitch stress
 - $\hat{\lambda}_o$ Optimal stretch for the maximum active stress
 - \hat{T} Characteristic time scale for contraction

S3.2 Elastomeric Substrate (\tilde{E} , $\tilde{\kappa}$)

Only two material constants (\tilde{E} , $\tilde{\kappa}$) are required to model the elastomeric substrates. The initial elastic modulus is directly specified by the manufacturer as $\tilde{E} = 1.5MPa$, while its incompressible behavior ($\tilde{\nu} = 0.49$) yields an initial bulk modulus of $\tilde{\kappa} = \frac{\tilde{E}}{3(1-2\tilde{\nu})} = 25MPa$.

S3.3 Cardiac Myocytes

The proposed model requires seven material-specific parameters ($\hat{\kappa}$, \hat{E}_c , \hat{E}_p , $\hat{\alpha}$, \hat{P} , $\hat{\lambda}_o$, \hat{T}) and two geometric-specific parameters ($\hat{\theta}$, $\hat{\lambda}_S$). Most of model parameters are available in the literature. The paper by Weiwad et al. (2000) provides in a single article nearly all the required test results to identify the material parameters entering into the proposed material model. Moreover, all their data are in a good agreement with similar test results for the heart muscle of adult rats (Granzier and Irving, 1995, Palmer et al., 1996 for passive behavior and Nishimura et al., 2000, Palmer et al., 1996 for active behavior). Thus, the test results presented in Weiwad et al. (2000) are used to identify five material-specific parameters entering into the proposed constitutive model.

In addition, experiments with length-wise cell alignment (Section 2) are used to identify the remaining three parameters; two experimental-conditions-specific parameters (\hat{P} , $\hat{\lambda}_S$) and the characteristic time scale of contractile behavior under the stimulating electric pulse (\hat{T}). Here, we assume that the cell conditions affect only the twitch stress \hat{P} and the pre-stretch $\hat{\lambda}_S$.

Isochoric Behavior of Intercellular Part (\hat{E}_c) and Isochoric Passive Behavior of Fiber Part (\hat{E}_p , $\hat{\alpha}$) Several researchers reported experimentally measured values for Young's modulus of non-activated rat cardiac myocytes by using atomic force microscopy (Lieber et al., 2004) or custom-designed force transducer (Weiwad et al., 2000). The measured values vary from $20kPa$ to $45kPa$ depending on the experimental protocols and the ages of rats. Following Weiwad et al. (2000), we use a Young's modulus, $\hat{E}_{passive} = 23kPa$ (see Fig. 3A). From Eq. (S16), recall that the measured Young's modulus of the non-activated cell can be decomposed into the contribution of intercellular part and passive fiber part. Here, we assume that the passive fiber part is mainly responsible for the passive elastic behavior, so that $\hat{E}_p = 21kPa$ and $\hat{E}_c = 2.3kPa$. Note that the passive stress ($T_{11}^{passive}$) can be expressed as:

$$T_{11}^{passive} = (T_{iso}^i)_{11} + (T_{ani}^{ip})_{11}, \quad (S21)$$

where using incompressibility each stress contribution can be determined from Eq. (S18) and Eq. (S19) assuming uniaxial loading conditions:

$$(T_{iso}^i)_{11} = \frac{\hat{E}_c}{3} \left(\bar{\lambda}^2 - \frac{1}{\bar{\lambda}} \right), \quad (S22)$$

$$(T_{ani}^{ip})_{11} = \frac{\hat{E}_p \bar{\lambda}}{\hat{\alpha}} \left[e^{\hat{\alpha}(\bar{\lambda}-1)} - 1 \right]. \quad (S23)$$

By curve-fitting the experimental results with the above equations (see Fig. 3B), we obtain $\hat{\alpha} = 5.5$.

Isochoric Active Behavior of Fiber Part (\hat{P} , $\hat{\lambda}_o$, \hat{T}) Weiwad et al. (2000) reported the evaluation of the isometric twitch stress as a function of calcium concentration (see Fig. 3B). Note that a constant calcium concentrations of $pCa = -\log_{10}(a_{Ca^{2+}}) = 2.74$ was used throughout the essay tests (Fig. 2) presented in Section 2. In order to get its overall dependence on the stretch, all the active tension-stretch relations are normalized by its maximum value, and then curve-fitted by the proposed quadratic form of active stress-stretch relation specialized to uniaxial loading:

$$(T_{ani}^{ia})_{11} = \begin{cases} \hat{P}q \left[1 - \left(\frac{\bar{\lambda} - \hat{\lambda}_o}{1 - \hat{\lambda}_o} \right)^2 \right], & \text{if } 1 < \bar{\lambda} < (2\hat{\lambda}_o - 1) \\ 0, & \text{otherwise} \end{cases} \quad (\text{S24})$$

As a result, we obtain $\hat{\lambda}_o = 1.24$, as shown in Fig. 3B. As described in Section 4, a range of values for the isometric twitch stress of $\hat{P} \in [2.8, 21.6]kPa$ is determined from experiments with length-wise cell alignment presented in Section 2. The characteristic contraction time can be determined by measuring the time when the signal reaches its maximum value after the activation starts. Fig. 3C shows a typical profile of the active amplitude history, and $\hat{T} = 0.21sec$ is determined.

Volumetric Behavior ($\hat{\kappa}$) For simplicity, we assume that the cardiac muscle is nearly incompressible and its volumetric behavior is determined by the passive response. Thus, using $\hat{E}_{passive} = 23kPa$ and $\hat{\nu} = 0.49$, we obtain a bulk modulus of $\hat{\kappa} = \frac{\hat{E}_{passive}}{3(1-2\hat{\nu})} = 380kPa$.

Isochoric Pre-stretch Behavior ($\hat{\theta}$, $\hat{\lambda}_S$) For the model parameter identification, the controlled test set (*i.e.*, the case with the length-wise cell alignment) with $\hat{\theta} = 0^\circ$ is used.

From the assay experiments in Section 2, we obtain $\hat{\lambda}_S \in [1.11, 1.18]$. Similar range of values for pre-stretch was also reported using a silicon substrate (Mansour et al., 2004).

S4 Parametric Studies

In this Section, we explore the effect of important parameters within MTFs with length-wise cell alignment such as the PDMS thickness, the isometric twitch stress of cells, the pre-stretch of cells, and the frequency of field-stimulation.

Effect of PDMS Thickness Here, the effect of PDMS thickness on the response of the MTFs is explored by varying \tilde{t} from $13.0\mu m$ to $28.0\mu m$. The average value of the two cell-condition-dependent parameters is used (*i.e.*, $\hat{\lambda}_S = 1.14$ and $\hat{P} = 9.0kPa$), while keeping all other parameters unchanged.

Fig. S1A shows the effect of PDMS thickness on the total curvature (K) of MTFs. As expected, an increase in PDMS thickness leads to a decrease in curvature. To quantify this behavior, the total curvature is decomposed into the passive contribution (K_p) and the active contribution (K_a):

$$K = K_p + K_a. \quad (\text{S25})$$

Fig. S1B reports the evolution of maximum passive and active curvature contributions (*i.e.*, $max(K_p)$ and $max(K_a)$) as a function of the PDMS thickness. The passive contribution of the curvature can be also estimated by applying a recent modification of the Stoney's equation

(Atkinson, 1995). Assuming that the layer of cells is much thinner than that of substrate, the Stoney *curvature* equation predicts the curvature of the bilayer film as

$$K_{stoney} = \frac{6(\hat{E}_c + \hat{E}_p) \ln \hat{\lambda}_S}{\tilde{E} \tilde{t}} \left(\frac{\hat{t}}{\tilde{t}} \right) \left(1 + \frac{\hat{t}}{\tilde{t}} \right). \quad (\text{S26})$$

The pre-stretched curvature predicted by (S26) is also reported in Fig. ??, and a good agreement with the passive contribution from the FEM calculations is observed.

Effect of Isometric Twitch Stress of Cells We vary \hat{P} from 0 to $30.0kPa$ while keeping all other parameters unchanged, including $\tilde{t} = 18.0\mu m$ and $\hat{\lambda}_S = 1.14$.

Fig. S1C shows the effect of isometric twitch stress on the curvature of MTFs. While the passive contribution of the curvature ($max(K_p)$) is unaffected by \hat{P} , the active contribution ($max(K_a)$) is observed to vary almost linearly with \hat{P} (Fig. S1D).

Effect of Cell Pre-stretch The effect of pre-stretch on the cardiomyocyte response is investigated by varying $\hat{\lambda}_S$ from 1.00 (*i.e.*, no pre-stretch) to 1.39 while keeping all other parameters unchanged and using $\tilde{t} = 18.0\mu m$ and $\hat{P} = 9.0kPa$.

Figure S1E reports the time history of film curvature for various level of cell pre-stretch. The results clearly show that the level of cell pre-stretch affects the curvature both during cell maturation and activation. Interestingly, for the active response, we observe a quadratic relation between the passive and the active curvature contribution. Thus, this study suggests that the maximum level of active response (*i.e.*, the maximum active mobility) for the MTFs can be achieved by introducing an optimal pre-stretch value. Moreover, Fig. S1F clearly show that the modified Stoney equation (*i.e.*, Eq. (S26)) largely underestimates the MTF curvature for large pre-stretch.

References

- W.J. Adams, T. Pong, N.A. Geisse, S.P. Sheehy, B. Diop-Frimpong, and K.K. Parker. Engineering design of a cardiac myocyte. *Journal of Computer-Aided Materials Design*, 14(1):19–29, 2007.
- A. Atkinson. *British Ceramic Proceedings*, 54(1), 1995.
- J.S. Bergström and M.C. Boyce. Constitutive modelling of the large strain time-dependent behavior of elastomers. *Journal of the Mechanics and Physics of Solids*, 46:931–954, 1998.
- W.F. Boron and E.L. Boulpaep. *Medical Physiology*. Saunders, 2009.
- M.A. Bray, S.P. Sheehy, and K.K. Parker. Sarcomere alignment is regulated by myocyte shape. *Cell Motility and the Cytoskeleton*, 65(8):641–651, 2008.
- O. Cazorla, J.-Y. Le Guennec, and E. White. Length-tension relationships of sub-epicardial and sub-endocardial single ventricular myocytes from rat and ferret hearts. *Journal of Molecular and Cellular Cardiology*, 32:735–744, 2000.
- A.W. Feinberg, A. Feigel, S.S. Shevkoplyas, S. Sheehy, G.M. Whitesides, and K.K. Parker. Muscular thin films for building actuators and powering devices. *Science*, 317(5843):1366–1370, 2007.
- H.L. Granzier and T.C. Irving. Passive tension in cardiac muscle: contribution of collagen, titin, microtubules, and intermediate filaments. *Biophysical Journal*, 68:1027–1044, 1995.
- J.-Y. Le Guennec, N. Peineau, J.A. Argibay, K.G. Mongo, and D. Garnier. A new method of attachment of isolated mammalian ventricular myocytes for tension recording: Length dependence of passive and active tension. *Journal of Molecular and Cellular Cardiology*, 22:1083–1093, 1990.
- S.C. Lieber, N. Aubry, J. Pain, G. Diaz, S.J. Kim, and S.F. Vatner. Aging increases stiffness of cardiac myocytes measured by atomic force microscopy nanoindentation. *AJP-Heart and Circulatory Physiology*, 287:H645–H651, 2004.
- H. Mansour, P.P. de Tombe, A.M. Samarel, and B. Russell. Restoration of resting sarcomere length after uniaxial static strain is regulated by protein kinase ϵ and focal adhesion kinase. *Circulation Research*, 94:642–649, 2004.
- S. Nishimura, S. Yasuda, M. Katoh, K.P. Yamada, H. Yamashita, Y. Saeki, K. Sunagawa, R. Nagai, T. Hisada, and S. Sugiura. Single cell mechanics of rat cardiomyocytes under isometric, unloaded, and physiologically loaded conditions. *AJP-Heart and Circulatory Physiology*, 287:H196–H202, 2000.
- R.E. Palmer, A.J. Brady, and K.P. Roos. Mechanical measurements from isolated cardiac myocytes using a pipette attachment system. *AJP-Cell Physiology*, 270:C697–C704, 1996.
- A.J.M. Spencer. *Continuum Theory of the Mechanics of Fibre-reinforced Composites*. Springer-Verlag, Wien-New York, 1984.
- W.K.K. Weiwad, W.A. Linke, and M.H.P. Wussling. Sarcomere length-tension relationship of rat cardiac myocytes at lengths greater than optimum. *Journal of Molecular and Cellular Cardiology*, 32:247–259, 2000.

F.E. Zajac. Muscle and tendon: Properties, models, scaling, and application to biomechanics and motor control. *Critical Reviews in Biomedical Engineering*, 17:359–411, 1989.

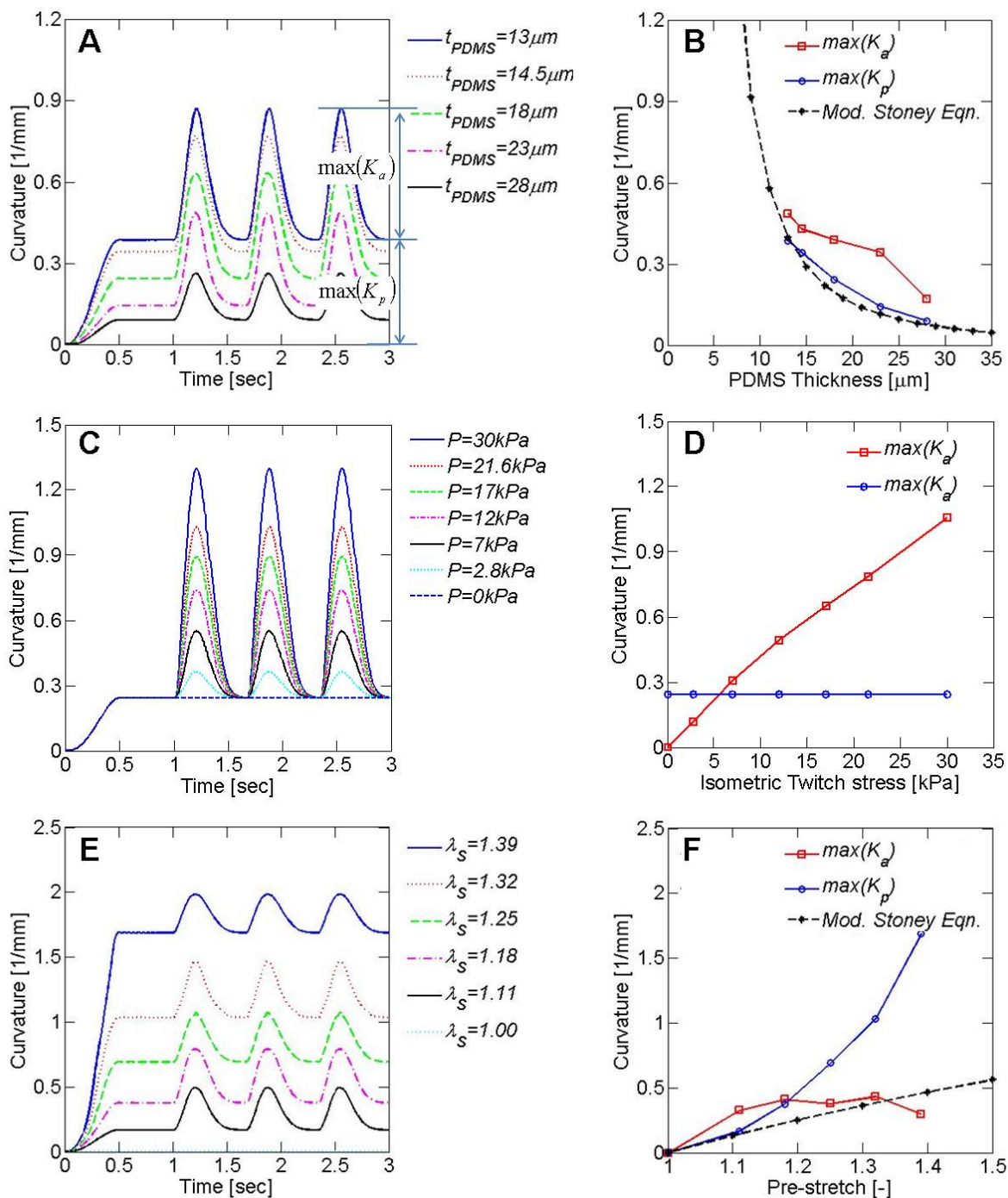


Figure S1: FE parametric studies: the left column for the time-curvature plots from FE analysis, and the right column for the curvature contribution of passive and active response ($\max(K_p)$ and $\max(K_a)$). (A-B) effect of PDMS thickness, (C-D) Effect of isometric twitch stress of cells, (E-F) effect of cell pre-stretch.